Desalination and Water Treatment
www.deswater.com

28 (2011) 239–246
April

1944-3994/1944-3986 © 2011 Desalination Publications. All rights reserved
doi: 10/5004/dwt.2011.1820

Numerical simulation of solar air heater with V-groove absorber used in HD desalination

Guangping Cheng*, Lixi Zhang

School of Engine and Energy, Northwestern Polytechnical University, Xi'an, Shaanxi, China 710072
Tel. +86-29-88492440; Fax +86-29-88495911; email: chengguangping@mail.nwpu.edu.cn

Received 25 January 2010; Accepted 4 January 2011

ABSTRACT

It is based on the heat transfer analysis of double-pass solar air heater with V-groove absorber, and used CFD software to make numerical simulation for the air flow paralleling with the V-groove in the air heater. The comparisons of simulation data with the experimental ones are made, it shows that the average difference between them is less than 8%, and the method of simulation is reliable. It is found by simulation that if the air flows across the V-groove in the air heater, the parameters of air heater, such as outlet air temperature, inlet-outlet pressure drop and efficiency of heat collected would be higher than the ones of parallel-flow under the same conditions; if the included angle of V-groove is increased, the inlet-outlet pressure drop of air in the heater would be decreased appreciably, and the outlet air temperature decreased obviously; if the height of V-groove is reduced about 10%, the inlet-outlet pressure difference of air in the heater would be reduced considerably, but the outlet temperature of it would be reduced seldom.

Keywords: V-groove; Parallel-flow; Cross-flow; Solar air heater; Numerical simulation; HD desalination

1. Introduction

Solar air heaters are main equipments used in agricultural products dehydration, architecture heated, HD desalination, and so on. So far, many theories, experiments, and numerical simulation researches of solar air heater have been carried out.

Flat plate heater is one kind of common air heaters. It has several advantages, such as simple structure, the ability of absorbing direct and scattered radiation simultaneously, etc. Now, the study of flat plate heater are mainly focused on reducing heat loss from its glass cover, using the higher selectivity absorbing coat, enhancing surface heat transfer of absorber plate, choosing the high transmittance and high intensity materials of its cover, etc.

Absorber plate is one of the main components of air heater, the shape of its surface is directly bound up with the property of heat absorbing and heat transfer. Bopche [1] had made some turbulators on absorbing plate, and concluded by experiments that it could enhance the heat transfer factor and friction factor by 2.82 and 3.72 times respectively than that of the plain absorber plate. Gupta [2] tested the properties of several absorber plates with different sizes of expanded metal mesh on it, and compared the test results with the flat absorber plate's ones, then the suitable roughness parameters of expanded metal mesh were determined. Esen, Ozgen [3–6] and their colleagues arranged aluminum cans on absorber plates in staggered and in order respectively in double-pass air heater. By experiments, it was showed that heat transfer between air and the surface of absorber plate was enhanced comparing with that without obstacles. The exergy analysis

*Corresponding author.

show that the largest irreversibility is occurring at the flat plate collector in which collector efficiency is smallest. Ho [7] studied the influence of recycle on performance of baffled double-pass flat plate solar air heaters with internal fins, the experiment had been performed that it can enhanced heat transfer rate, but the flow resistance and energy cost were increased. The thermal performance of a double-glass and double-pass solar air heater with a packed bed above the heater absorber plate was experimentally and theoretically investigated by Ramadan [8], the influence of mass flow and porosity of the packed bed material on the performance of heater were also studied, it was advisable to use the packed bed materials which have higher density and lower porosities, furthermore, recommended to operate the system with packed bed at 0.05 kg/s or lower to have a lower pressure drop in the system. An experimental studies for flat plate, finned and V-groove air heaters by Karim [9], V-groove heater was found to be the most efficient, whereas, the flat plate heater was the least efficient, the double-pass air heater lead to a further improvement comparing to single pass one. The mathematical models of heaters, such as with the V-plate, flat plate, single air pass, double air pass, and with or without fins were given by Yuan [10], as well as the instantaneous efficiency computing methods. A numerical investigation of turbulent forced convection in a two-dimensional channel with periodic transverse grooves on the wall of lower channel was conducted by Eiamsa-ard [11], in order to investigate the influence of turbulence models on the results, computations based on a finite volume method were carried out by utilizing four turbulence models: the standard k–ε, the renormalized group (RNG) k–ε, the standard k–ω, and the shear stress transport (SST) k–ω turbulence models. The predicted results of using several turbulence models indicated that the RNG and k–ε turbulence models generally provide better agreement with available measurements than others, so the k–ε turbulence model was choose to simulate the complex flow. The results were shown that the heat transfer rate of absorber with rectangle was 1.58 times than the smooth plate. Kumar [12] used the Fluent software to simulate the rough absorber plate, the results were that the k–ε (RNG) model was good at evaluating this kind of plates and the friction coefficient of it, and it can given the optimal value finally.

The V-groove plate has many advantages, such as it can reflect the incident light many times, absorbs the energy converted from the light, and increases the heat transfer area between air and absorber. Therefore, in order to study the property of the V-groove double-pass solar heater in this paper, the CFD software is used to simulate the air heaters under different flow state and different V-groove structures separately, the results can be referenced for this kind of solar air heater's design.

2. Analysis of structure and heat transfer

2.1. Structure and parameters

The shape of the V-groove double-pass solar air heater is rectangular block with V-groove heat absorbing plate in it. Its structure is shown in Fig. 1.

To compare the simulation results with the test data from the literature [9] and to validate the accuracy of the numerical simulation, the structure parameters that are the same as the experiment ones are used in simulation. The parameters are: the length of the absorbing plate is 1.9 m, the width of it is 0.7 m; the height of V-groove is 5 cm, the thickness of it is 1 mm, the included angle is 60°, the material is stainless steel; the air inlet section of heater is 0.0175 m^2.

2.2. Heat transfer network

For solar air heater, as the sun light passes through its glass cover(c), most part of the energy is absorbed by the V-groove, and converted to heat.

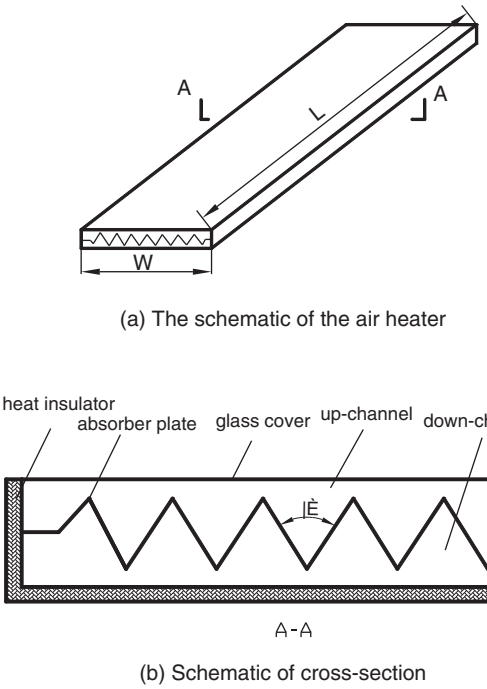

(a) The schematic of the air heater

(b) Schematic of cross-section

Fig. 1. Schematic of the air heater and its cross-section.

When the air flow enters the air heater, it firstly enters into the up-channel, and makes a convection heat transfer with V-groove and glass cover, then flows into the down-channel, also makes a convection heat transfer with V-groove and the insulation bottom board (b). Meanwhile, V-groove transfers heat with (c) and (b) respectively by radiation because of the temperature difference between them. The heat dissipates into the environment by the convection and radiation between the glass cover (c) and ambient air (a). The coefficient of total heat loss is U_t. It is the same as the convection and radiation heat transfer exists between (b) and (a), the coefficient of total heat loss is U_b.

To analyze the heat transfer network in double-pass air heater, taking the parallel flow as an example, the transfer network is shown in Fig. 2.

For every node of the heat transfer network in Fig. 2, the energy balance equations can be written under steady working state. The temperature T_c, T_p, T_b can be calculated by the methods provided in literature [11].

In the energy balance equations, the heat transfer coefficient between heat absorber and air, the coefficient between air and glass cover, etc., should be calculated by program, in which the heat transfer formulas are used.

For convenience, based on the finite volume method, the fluid and heat transfer simulation software is used to acquire the heat transfer performance of the air heater.

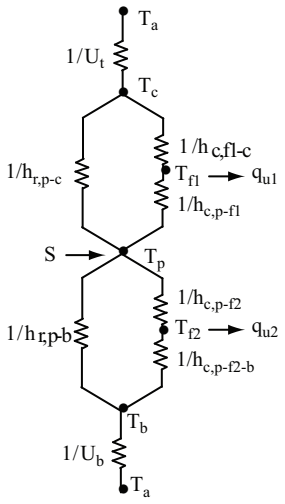

T—temperature, K; *h*—coefficient of heat transfer, W/(m².K); *U*—coefficient of heat loss, W/(m².K); *S*—the actual absorbing radiation energy, W/m². The subscripts: *g*—the glass cover; *P*—V-groove absorber; *b*—insulation bottom board; *α*—air; *f1,f2*—the air flows in the up-channel and down-channel; *c*—convection heat transfer; *r*—radiation heat transfer; *t*—total radiation and convection heat transfer.

Fig. 2. Heat transfer network of solar air heater.

3. Numerical simulation for flow field of air heater

Taking account of the turbulent flow of air in the collector, the standard *k*– ε model of fluent software is adopted. To facilitate the calculation of the heat transfer performance of collector in different structures and different flow patterns, the finite volume method is used to disperse the whole flow field of collector and the heat-absorbing plate.

3.1. Control equations

The basic control equations for flow field calculation include continuity equation, momentum equation and energy equation. All above equations are in Reynolds-averaged equation forms. In the Cartesian coordinates, the mass conservation equation is:

$$\frac{\partial \rho}{\partial t} + \frac{\partial}{\partial x_i}(\rho U_i) = 0 \tag{1}$$

In this equation, U_i is correspond to the average velocity of x, y, z direction respectively, ρ is average density.

Momentum conservation equation is:

$$\frac{\partial(\rho U_i)}{\partial t} + \frac{\partial(\rho U_i U_j)}{\partial x_j} = -\frac{\partial P}{\partial x_i} + \frac{\partial}{\partial x_j}\left(\mu_i \frac{\partial U_i}{\partial x_j} - \rho \overline{u_i u_j}\right) \tag{2}$$

Here, i, j = 1, 2, 3, P represents average pressure, $\rho\overline{u_i u_j}$ represents Reynolds stress tensor. From Buossniesq's hypotheses, the relationship between Reynolds stress and time averaged velocity gradient is:

$$-\rho \overline{u_i u_j} = \mu_i \left(\frac{\partial U_i}{\partial x_j} + \frac{\partial U_j}{\partial x_i}\right) - \frac{2}{3}\left(\rho k + \mu_i \frac{\partial U_i}{\partial x_j}\right)\delta_{i,j} \tag{3}$$

In this equation, μ_i is turbulent viscosity coefficient, k is turbulent kinetic energy, this two parameters can be solved by turbulent model equations.

Energy conservation equation is:

$$\frac{\partial(\rho T)}{\partial t} + \frac{\partial(\rho U_j T)}{\partial x_j} = \frac{\partial}{\partial x_j}\left(\Gamma \frac{\partial T}{\partial x_j} - \rho \overline{u_j \theta}\right) + \frac{1}{C_p}(\Phi + \dot{q} - \nabla \cdot q_r) \tag{4}$$

In above equation, T represents average temperature, Γ is effective heat transfer coefficient, $\rho\overline{u_j\theta}$ is turbulence heat flow. The energy equation is an energy balance relationship comprehensive taking account of the thermal conductivity, convection and radiation. In the last item of Eq. (4), the Φ, $\dot{q}$ and $\nabla \cdot q_r$ represent the source items of heat flow produced respectively by viscous dissipation, burning and radiation.

Additional scalar equations include k equation:

$$\frac{\partial(\rho k)}{\partial t} + \frac{\partial(\rho k u_i)}{\partial x_i} = \frac{\partial}{\partial x_j}\left[\left(\mu + \frac{\mu_t}{\sigma_k}\right)\frac{\partial k}{\partial x_j}\right] + G_k + G_b - \rho\varepsilon \tag{5}$$

Equation:

$$\frac{\partial(\rho\varepsilon)}{\partial t} + \frac{\partial(\rho\varepsilon u_i)}{\partial x_i} = \frac{\partial}{\partial x_j}\left[\left(\mu + \frac{\mu_t}{\sigma_\varepsilon}\right)\frac{\partial \varepsilon}{\partial x_j}\right] + C_{1\varepsilon}\frac{\varepsilon}{k}(G_k + C_{3\varepsilon}G_b) - C_{2\varepsilon}\rho\frac{\varepsilon^2}{k} \tag{6}$$

In the two equations, G_k represents the turbulence kinetic energy caused by the laminar flow gradient; G_b is the turbulence kinetic energy caused by buoyant force; Y_m is fluctuation caused by the transitive diffusing in a compressed turbulence flow; C_1, C_2 and C_3 are constants, σ_k and σ_ε are the Prantl turbulence numbers of k and ε equations.

Turbulence swirl viscosity μ_t is determined by the following formulas:

$$\mu_t = \rho C\mu \frac{k^2}{\varepsilon} \tag{7}$$

The constants in the model are: $C_{1\varepsilon} = 1.44$, $C_{2\varepsilon} = 1.92$, $C\mu = 0.09$, $\sigma_k = 10$, $\sigma_\varepsilon = 1.3$.

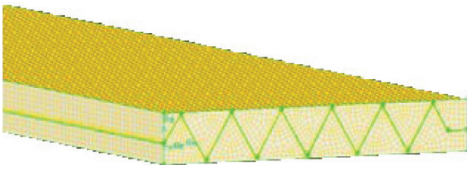

(a) Flow field and V-groove

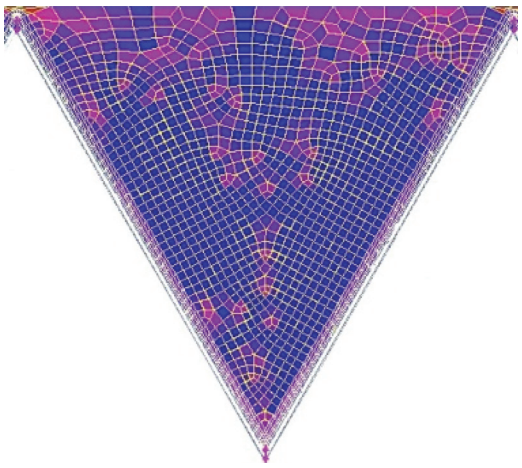

(b) Meshes in V-groove

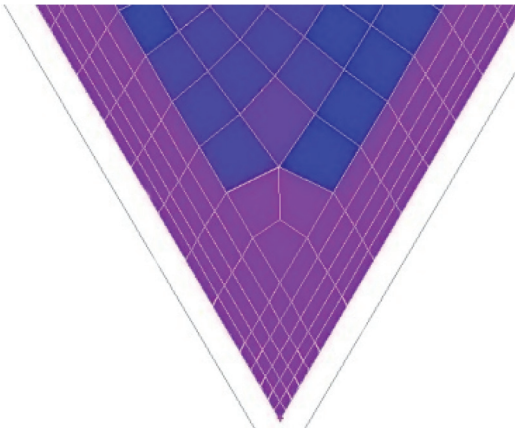

(c) Local meshes of V-groove

Fig. 3. Calculation model.

3.2. Computational modeling and meshing

To establish computational model for the flow field of parallel flow in the collector, Gambit software is used to plot meshes, as shown in Fig. 3. The structured hexahedron gridding is adopted for the whole control volume. To ensure the accuracy of calculation, non-homogeneous structured meshes are plotted on the boundary layers of the V-groove heat-absorbing plate, and the density of meshes is increased near the boundary of V-groove. The size of the first layer of meshes close to the boundary is 0.5 mm, then the size of meshes increases at the rate of 1.2 layer by layer. The meshes in the airflow direction are plotted equably. The distance between two near mesh is 5 mm.

If the number of meshes increased by 1/3 times, which is about 53×10^4. It's shown that the calculation results of former and later are almost the same.

Therefore, the meshes are independent. The needed number of meshes is about 40×10^4.

3.3. Boundary conditions

The numerical simulation calculation of the double-pass air heater with V-groove absorber involves convection heat transfer between air and the surface of V-groove, and the heat conductivity inside the V-groove. This problem is the one of conjugated heat transfer between fluid and solid. The effective method to solve it is to disperse the entire control regions and the different heat transfer processes in various regions, and then to combine them to solve it. But the generalized coefficient of diffusion and the generalized source item in general control equations of different regions are not the same, therefore the coupled interfaces are transferred to the inner regions in calculation.

During the calculation, the item S, which is the effective solar energy absorbed by heat-absorbing plate, is transferred to be the source item. For the absolute temperature of V-groove, glass cover and bottom board are not very higher, so the radiation heat transfer between V-groove and glass cover, V-groove and bottom board, ambient air and glass cover, ambient air and bottom board are ignored respectively. The effects of air viscosity on the pressure losses are considered, and the default value for air viscosity in the software is used.

The heat produced by unit volume is calculated by the following formula [13]:

$$\dot{F} = \frac{G_\tau (ta)_e A_C}{v} \tag{8}$$

Here, $\mathbf{G}_T$ is solar radiation intensity, W/m^2; $(\tau\alpha)_e$ is the product of effective transmissivity and effective absorption rate of solar radiation, taking 0.87; A_c is the effective heat absorption area of collector, m^2; v is volume of the collector, m^3.

To research the energy losses of air fluid passing through the air heater, the air is considered as ideal gas, and the relationship of its P, V and T can be calculated by ideal gas state equation.

3.4. Solving the control equations

In each control equation, the first order of dispersion form is adopted by the variables and the coupling methods of pressure-velocity and the simple algorithm are used by solver. The default relaxation factors in the software are adopted. The residuals of each variable are set as 1×10^{-4}. If the process of calculation is not convergence, the relaxation factors can be adjusted smaller properly.

4. Numerical simulation

4.1. Simulation and comparison for parallel flow

The experimental conditions provided by literature [9] are under clear sky, between 2 h before and 2 h after of solar noon. The air flow rate and inlet air temperature were not changed. The collector slope was 10°. The solar irradiation must be above 630 W/m^2, the fluctuation of it was less than 50 W/m^2. The wind speed across the collector was less than 4.5 m/s, etc.

To insure the numerical simulation and experiment under the same conditions, according to the parameters of experiments, the temperature of air entering the collector is taken as 312 K, the frames and bottom of collector are viewed as insulated in the simulation.

The expression of convection heat transfer coefficient between glass cover and ambient air was offered by the literature [13], it was $h_w = 2.8 + 3.0\ V$, here, V was the wind speed. As V = 4.5 m/s, h_w = 16.3 W/(m$^2\cdot$°C); V = 2.5 m/s, h_w = 10.3 W/(m$^2\cdot$°C). The expression of h_w is also suitable to use in the inclination cover. For the wind speed under experimental condition was not supplied detailed by the literature [9], so that h_w was approximately taken as 10 W/(m$^2\cdot$°C) in the numerical simulation referencing other test data at lower wind speed [13].

As the solar radiation is constant, the outlet air temperatures of simulation and test ones from the literature [9] of air heater are shown in Fig. 4. It indicates: as the mass flow of air increases, the outlet temperature

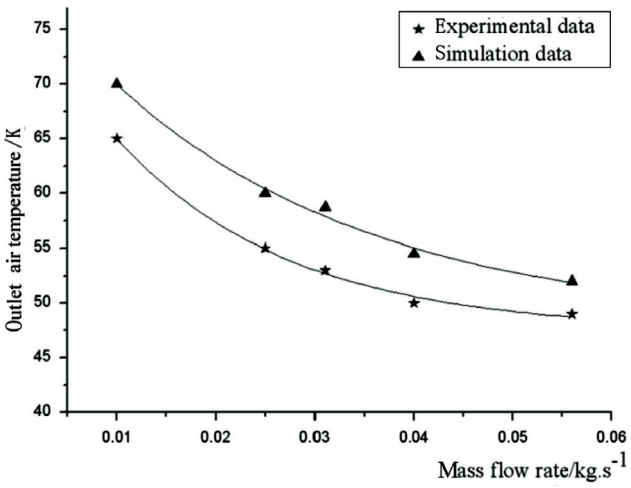

Fig. 4. Outlet temperatures changed with air mass flows.

decreases; the simulation data are greater than the test ones. The maximum error between the simulation data and the test ones is 8.2%, the average error between them is 5.2%.

As the mass flow is 0.031 kg/s, and the other parameters are not changed, the air temperature differences between the outlet and the inlet of air heater changed with the radiation intensity are shown in Fig. 5. The results show: as the radiation intensity increases, the differences of temperature between the outlet and the inlet are increased; the biggest error between them is 5.2%, and their average error is 4.3%.

In above comparisons, the errors between simulation data and test ones are mainly caused by the testing errors, the accuracy of supposed solar energy values absorbed by the V-groove, the deviation of heat transfer coefficient between the cover and the ambient air, the ignored radiation heat transfer in the simulation calculation, and so on. It is known from the comparisons that the simulation results are basically consistent with the experimental ones, that mean the boundary conditions assumed in simulation for the fluid-solid coupling model are basically right, and the simulation method could be applied to predict the performance of air heaters under similar conditions.

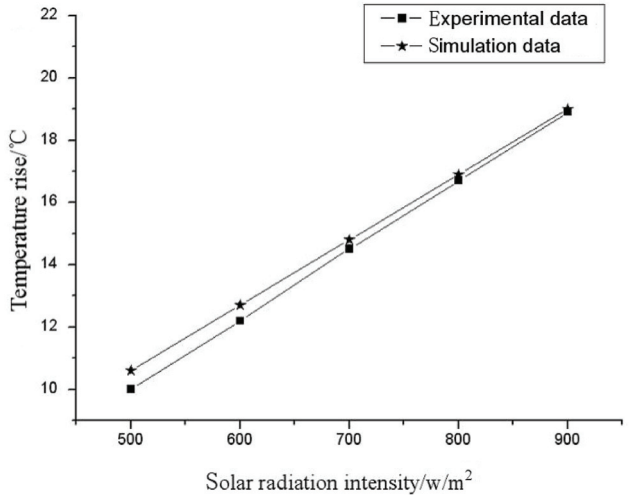

Fig. 5. Outlet-inlet temperature differences changed with solar radiation intensities.

4.2. Comparison of cross-flow with parallel –flow

In order to compare the performance differences of cross-flow with parallel-flow in the air heater, supposing the size, the material, and the boundary of absorber plate are the same under various simulation conditions, only the direction of air flow is changed.

As the mass flow is 0.031 kg/s, and the solar radiation intensity is 600 W/m^2, the simulated temperature field of the parallel-flow and the cross-flow are shown respectively in Fig. 6 and Fig. 7. The two figures indicate that the temperatures of absorber plate in cross-flow are lower than the corresponding ones in parallel-flow. The reason is that: the turbulence is formed in the V-groove under the cross-flow, so the heat transfer rate between absorber plate and air is enhanced; meanwhile the inlet-outlet pressure drop of air is increased too. The pressure drop of air in cross-flow is 3 Pa higher than that of parallel-flow by simulation.

The velocity fields of simulation for above two flow types are shown in Fig. 8 and Fig. 9 respectively. Fig. 10 shows the comparison of the inlet-outlet temperature rise in air heater under different solar radiation intensities. It indicates that the temperature rise of simulation for

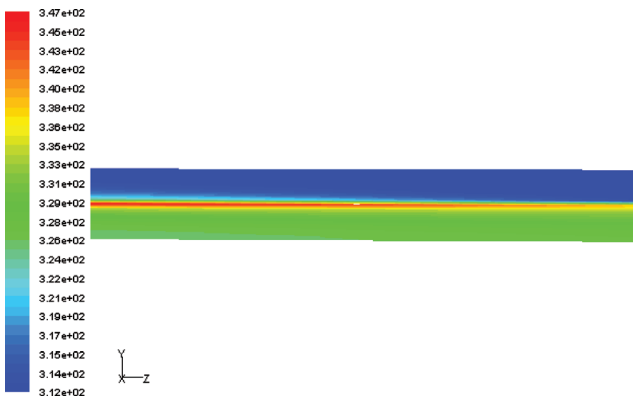

Fig. 6. Temperature field of parallel-flow.

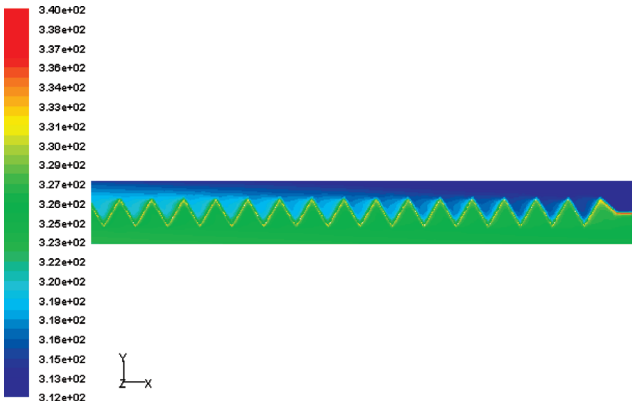

Fig. 7. Temperature field of cross-flow.

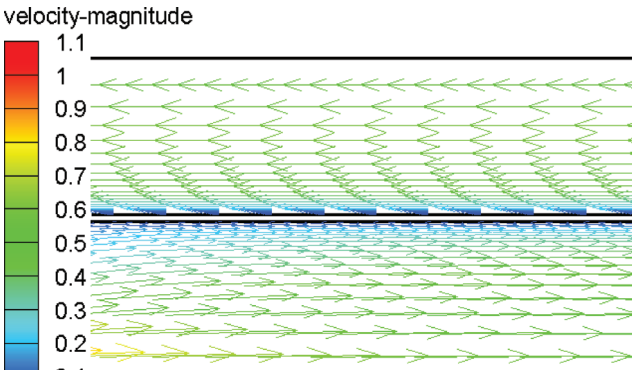

Fig. 8. Velocity vectors of parallel-flow.

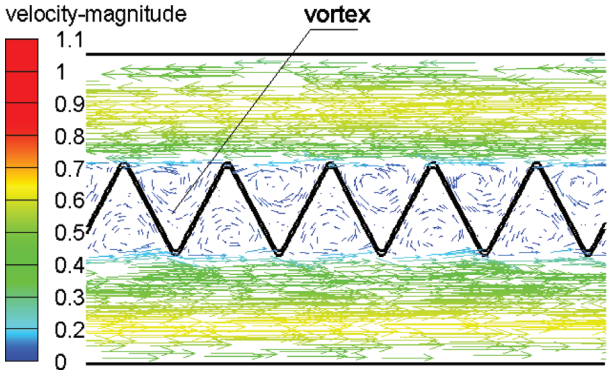

Fig. 9. Velocity vectors of cross-flow.

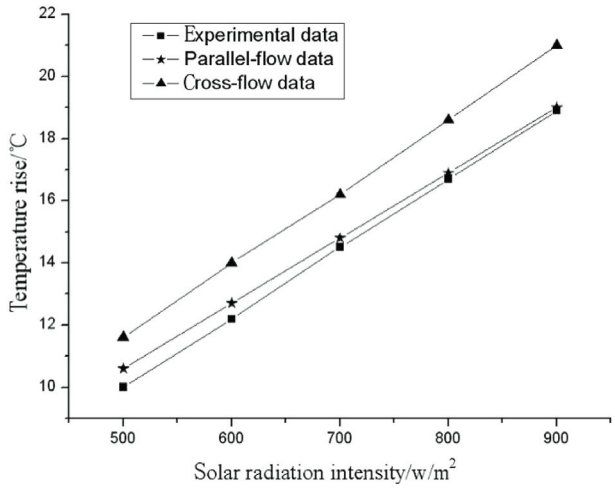

Fig. 10. Temperatures changed with solar radiation intensities.

parallel-flow is a little higher than the experimental value; the temperature rise of the cross-flow is higher than that of the parallel-flow under the same condition. It means that the solar collecting efficiency of the cross-flow is higher than that of the parallel-flow.

4.3. Simulations for different absorbers' included angles

The included angle θ of the V-groove absorber is shown in Fig. 11. If θ is changed, the influence of flow resistance and heat transfer rate on the cross-flow in air heater would be more obviously than that on the parallel-flow.

Fig. 11 shows the relation of outlet air temperatures and outlet-inlet pressure drops changed with θ. The outlet temperature of air heater decreased with θ increased. When θ is increased from 60° to 120°, the outlet temperature is decreased about 9K. The reason is that the larger θ of the V-groove in the same of area is, the less surface of heat transfer is; the weaker disturbance from the V-groove to the air flow is, the lower of the heat transfer rate is.

The pressure drop would be decreased with θ increased. As θ is increased from 60° to 120°, the pressure drop is decreased by 1.4 Pa. For the larger of θ is, the less flow resistance of V-groove to air is.

In a word, the outlet temperature of air heater decreased obviously, while the pressure drop decreased a little with θ of V-groove increased.

4.4. Numerical simulation of the V-groove height changed

To reduce the air pressure drop in cross-flow state, it could be considered to reduce the height of the V-groove.

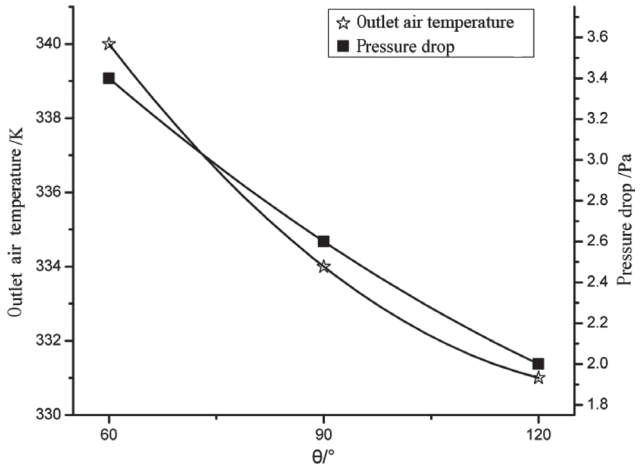

Fig. 11. Outlet air temperatures and outlet-inlet pressure drops changed with θ.

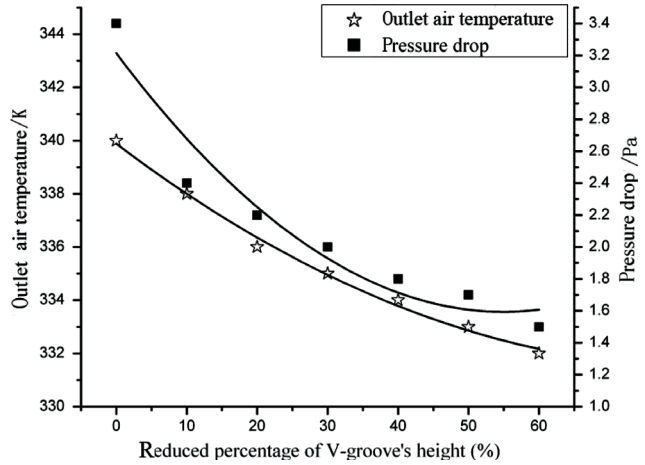

Fig. 12. Outlet air temperatures and outlet-inlet pressure drops changed with V-groove's heights.

It is assumed to reduce the height of the V-groove from 10% to 60% separately under the same boundary and initial conditions, and to simulate its flow field of cross-flow with the CFD two-dimension model. The simulation results are shown in Fig. 12.

Fig. 12 indicates that the air temperature in the outlet of heater reduced with the decrease of the height of V-groove. The reason is that: as the height of V-groove is decreased, the disturbing for the air flow by the sharp angle of V-groove is decreased gradually. Meanwhile, the air flow section is increased, the flow rate and the heat transfer coefficient are reduced, therefore, its outlet temperature is decreased.

When the height of the V shape decreased by 10%, the pressure drop decreased larger, it is about 1.1 Pa, it indicates that the sharp angle of the V-groove has a large resistance to the fluid. As the reducing percentage of the V-groove's height is increased, the surface of absorbing plate tends to gentle, so the pressure drop is decreased slowly. When the height of V-groove is reduced from 10% to 60% of total height, the pressure drop is about 0.7 Pa.

5. Conclusion

Using the standard $k-\varepsilon$ model in fluent software and the liquid-solid couple calculation method, it is predicted the flow properties of double-pass solar air heater with the V-groove absorber accurately in this paper. From the simulation results of this study, the heat transfer effect in air cross-flow state is higher than that in the parallel-flow state. When the height of V-groove is reduced by 5~10%, the air flow resistance in air heater reduces obviously. So it is suggested to use the cross-flow state and the reduced height of V-groove when it is necessary to use double-pass solar air heater with V-groove absorber.

Acknowledgement

This work is supported by graduate starting seed fund of Northwestern Polytechnical University, and natural science fundamental research project of shaanxi province under the project No: 2007$E_2$27.

References

[1] S.B. Bopche and M.S. Tandale, Experimental investigations on heat transfer and frictional characteristics of a turbulator roughened solar air heater duct, Int. J. Heat Mass Transfer, 52 (2009) 2834–2848.
[2] M.K. Gupta and S.C. Kaushik, Performance evaluation of solar air heater having expanded metal mesh as artificial roughness on absorber plate, Int. J. Thermal Sci., 48 (2009) 1007–1016.
[3] F. Ozgen, M. Esen and H. Esen, Experimental investigation of thermal performance of a double-flow solar air heater having aluminium cans, Renewable Energ., 34 (2009) 2391–2398.
[4] H. Esen, Experimental energy and exergy analysis of a double-flow solar air heater having different obstacles on absorber plates, Build. Environ., 43 (2008) 1046–1054.
[5] H. Esen, F. Ozgen, M. Esen and A. Sengur, Modelling of a new solar air heater through least-squares support vector machines, Expert Syst. Appl., 36 (2009) 10673–10682.
[6] H. Esen, F. Ozgen, M. Esen and A. Sengur, Artificial neural network and wavelet neural network approaches for modelling of a solar air heater, Expert Syst. Appl., 36 (2009) 11240–11248.
[7] C.D. Ho, H.M. Yeh and T.W. Cheng, The influences of recycle on performance of baffled double-pass flat-plate solar air heaters with internal fins attached, Appl. Energ., 86 (2009) 1470–1478.
[8] M.R.I. Ramadan and A.A. El-Sebaii, Thermal performance of a packed bed double-pass solar air heater, Energy, 32 (2007) 1524–1535.
[9] M.A. Karim and M.N.A. Hawlader, Development of solar air collectors for drying applications, Energ. Convers. Manage., 45 (2004) 329–344.
[10] X.D Yuan, M T and S.Y. Huang, Numerical simulation of the heat transfer for the v-type air heater, J. Huazhong Univ. Sci. Technol., 29(10) (2001) 86–89.
[11] S. Eiamsa-ard and P. Promvonge, Numerical study on heat transfer of turbulent channel flow over periodic grooves, Int. Commun. Heat and Mass Transfer, 35 (2008) 844–852.
[12] S. Kumar and R.P. Saini, CFD based performance analysis of a solar air heater duct provided with artificial roughness, Renewable Energ., 34 (2009) 1285–1291.
[13] H.F. Zhang, Solar thermal utilization and computer simulation, Xian: Press of Northwestern Polytechnical University, (2004) 60–127.